13-0111

Earth's low degree gravitational variations from space geodetic data

V. Luceri (1), C. Sciarretta(1), G. Bianco(2)
(1) e-GEOS S.p.A., Centro di Geodesia Spaziale, Matera, Italy
cinzia.luceri@e-geos.it, cecilia.sciarretta@e-geos.it
(2) Agenzia Spaziale Italiana, Centro di Geodesia Spaziale, Matera, Italy
giuseppe.bianco@asi.it

Abstract. *Geodetic techniques allow monitoring the main mass variations of our planet reflected by variations of the Earth's figure axis and oblateness which are described by the second-degree geopotential coefficients. SLR data have been used in this study to retrieve time series of direct estimates of low degree geopotential coefficients using 7 geodetic satellites: Lageos1, Lageos2, Stella, Starlette, Ajisai, Etalon1 and Etalon2.*
SLR, GPS and VLBI can be used to estimate these variations through derived excitation functions from the EOPs estimations. The excitation functions incorporate the influence by earth's atmosphere and oceans, both from their mass and motion components, which can be modelled by the atmospheric and oceanic angular momenta variations provided by the IERS dedicated bureaus.
The $C_{21}/S_{21}/C_{20}$ long-term geodetic time series, obtained with different methods and using different data, deprived of the modelled atmospheric and oceanic 'motion' terms to isolate their response to the mass variations only, are presented and inter-compared, to evaluate their consistency. The residual signal contents of the geodetic values are evaluated too.

Introduction

The redistribution of the mass within the earth system induces changes in the Earth's gravity field. Due to the long record of accurate and continuous laser ranging observations to Lageos, Starlette and other geodetic satellites, Satellite Laser Ranging (SLR) is the only current space technique capable to monitor the long time variability of the Earth's gravity field with adequate accuracy. In particular, this study is focused on the variations of the second-degree Stokes coefficients related to the Earth's principal figure axis and oblateness: C_{21}, S_{21} and C_{20}. On the other hand, surface mass load variations induce excitations in the EOP that are proportional to the same second-degree coefficients. Time series obtained from direct estimation, together with those derived from the EOPs, can be very helpful to describe the mass redistribution process on a global scale.

Direct estimations from SLR

SLR observations of a constellation of seven geodetic satellites (Stella, Starlette, Ajisai, the two Lageos, and the two Etalon) acquired by the worldwide network from 1984 to May 2013, have been analyzed to produce a time series of the estimated variations in the low degree geopotential coefficients. All the satellites considered in the analysis have spherical shapes in order to minimize the non-gravitational forces, their inclinations range from 50 to 190 degrees and their altitude from 800 to 19,000 km. The analysis procedure follows two sequential steps: 1) the computation of many arc solutions in which each satellite orbit is piecewise reduced, and 2) their combination in a unique multi-year solution, respectively using the software packages Geodyn II and Solve developed at the NASA Goddard Space Flight Center.
The adopted analysis models follow the IERS Convention 2010 (Petit et al, 2010) and the main differences in the analysis approach for the various satellites stay on the definition and estimation of

the orbit parameters. For each satellite we have adopted ad-hoc arc lengths and models in order to achieve the best orbit determination for each of them. The normalized geopotential coefficients C_{20}, C_{21} and S_{21} have been estimated every 30 days. The time series have been subsequently processed to remove signals due to known effects: the anelastic frequency dependent tidal correction according to the Eanes model (Eanes, 1995) for C_{20}, and the solid earth and ocean pole tide for C_{21} and S_{21}, applied according to the IERS conventions 2010.

The pole tide is generated by the centrifugal effect of polar motion. The deformation on solid earth and oceans induce variations in the C_{21} and S_{21} coefficients, at the annual and Chandler wobble frequencies. The largest effect is due to the solid earth pole tide, roughly 6 times larger than the ocean pole tide for C_{21} and 8 times for S_{21}. Modeling the ocean pole tide makes the signal at the Chandler wobble frequency negligible, while reducing the annual signal by 83% in C_{21} and 27% in S_{21}.

The seasonal signals were not removed in order to be comparable with the series from EOP. The full coefficient time series is available from 1984 to May 2013 but the investigation is focused on the estimates after 1993, when the full SLR satellite constellation became available. The dynamics SLR series will be referred as DSLR in the following.

Figure 1. shows the time series variations after 1993. An annual component, with variable amplitude, is evident in the ΔC_{21} and ΔS_{21} series; annual and semiannual components are present in the ΔC_{20} series.

An assessment of the values has been made using the coefficients estimated by the University of Texas Center for Space Research (CSR) and available with the GRACE Release 5 products RL05 (Cheng et al, 2011).

The CSR series is represented by small circles in Figure 1. and the two estimates clearly show similar variations, at similar periods and with similar amplitudes.
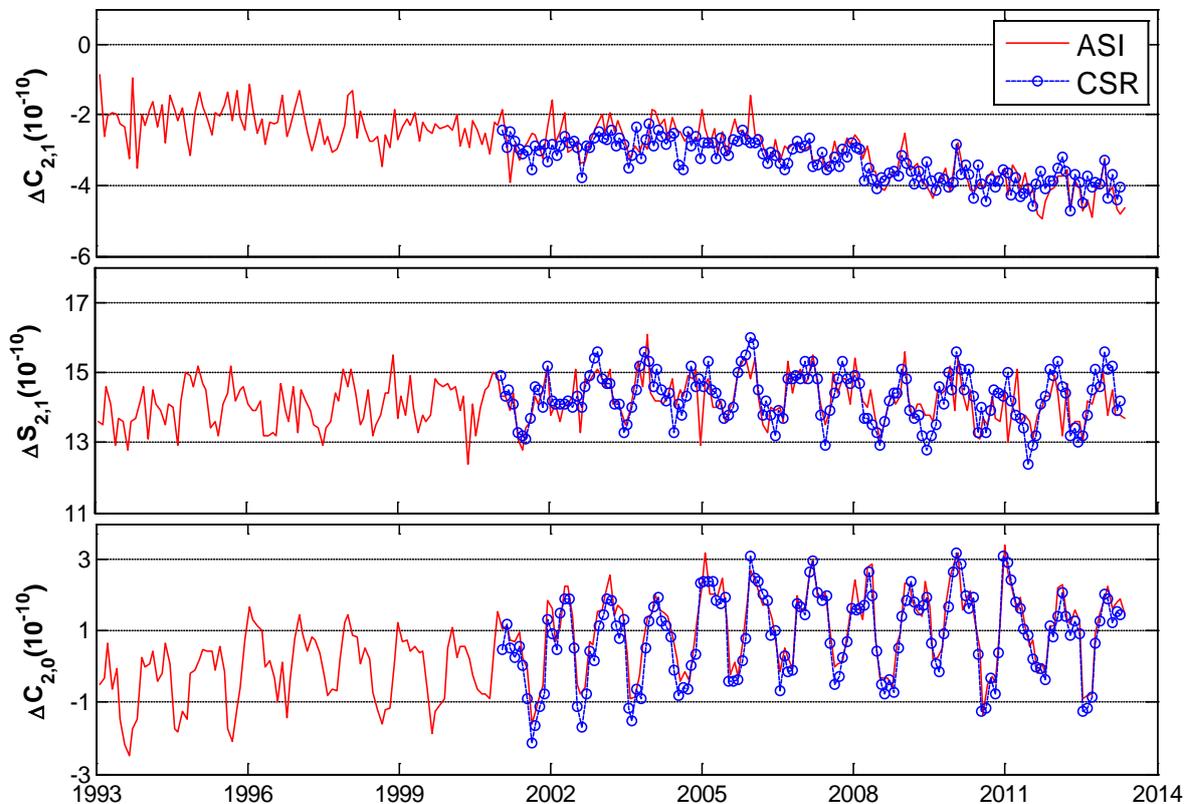

Figure 1. ΔC_{21}, ΔS_{21} and ΔC_{20} time series estimated by ASI (line) and CSR (circles)

EOP derived C_{21}, S_{21} and C_{20} variations

The CGS 3-day SLR EOP estimations (x, y, LOD), from 1983 onwards, and the CGS VLBI EOP estimations at session epochs, from 1984 onwards, have been transformed into excitations following the algorithm introduced by Wilson and Vicente [2002] , using the Chandler term period T = 433d and its quality factor Q = 175.

The Geophysical excitation functions (mass and motion terms) from the Atmospheric Angular Momentum Functions are provided by AER, Atmospheric and Environmental Research (aamf.ncep.reanalysis, Salstein et al., 1993, 1997, 2005; Zhou et al., 2006), acting as Special Bureau for Atmosphere in the IERS Global Geophysical Fluid Center. The wind terms are computed by integrating winds from the Earth surface to 10 hPa, the top of atmospheric model.

The Geophysical excitation functions (mass and motion terms) from the Oceanic Angular Momentum (OAM) Functions come from the most updated ECCO_kf080.chi values (from 1993 up to June 2012) by ECCO, "Estimating the Circulation and Climate of the Ocean" provided by NASA/JPL, acting as Special Bureau for Oceans in the IERS Global Geophysical Fluid Center. The ocean model used to compute the OAM is forced by atmospheric fields from the NCEP/NCAR Reanalysis Project, i.e. it is coherent with the Atmospheric excitation functions taken into account.

The geophysical "motion" contribution (atmospheric winds + oceanic currents) from 1993 onwards is plotted in Figure 2. together with the geodetic excitations from VLBI and SLR EOPs (EOPV and EOPS onwards). To better highlight signal features at the annual and semi-annual scale, a 90-day running mean has been computed on the CGS EOPS and EOPV values, and on the geophysical motion-only excitation components, after having averaged the AER atmospheric wind term excitations, provided four times a day, into daily values. The plots show the 90-day running mean values; average values have been removed from all the series in the plots.
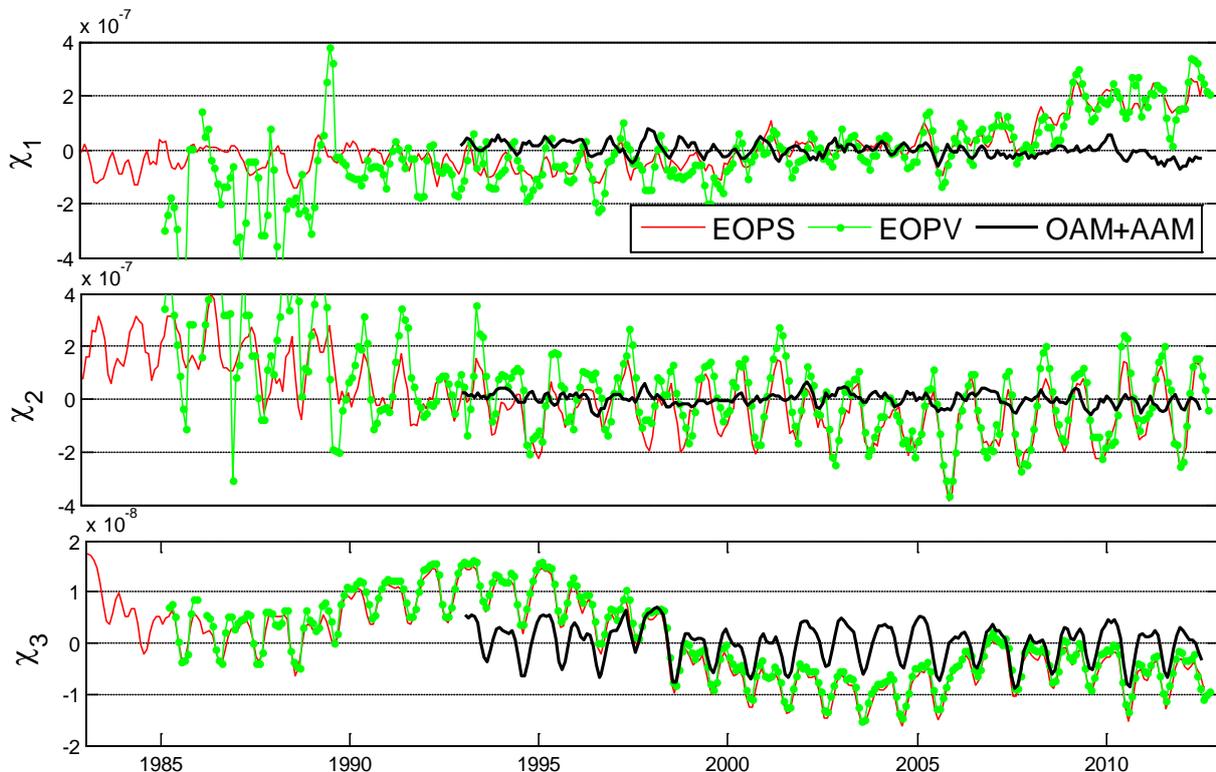

Figure 2. Polar motion and LOD excitations. EOPS is the SLR EOP excitation, EOPV is the VLBI EOP excitation, OAM+AAM is the geophysical excitation (motion part only)

The geophysical motion component clearly induces low-medium frequency signatures (1-4 cycles per year) in the C_{20} variations, originating a significant percentage of its variance, while the low-

medium frequencies visible in the EOPS and EOPV C_{21}/S_{21} variations have their origin in other forcing terms.

According to Chen et Wilson [2003], normalized C_{21}, S_{21} and C_{20} variations can be derived from the EOP mass load excitation functions, in turn computed for each component as $\chi_{mass} = \chi_{geodetic} - (\chi^{OAM}{}_{current} + \chi^{AAM}{}_{wind})$ by means of the following equations:

$$\Delta C_{21} + i\Delta S_{21} = -(1+k_2')\sqrt{\frac{3}{5}}\frac{(C-A)}{1.098R^2M}(\chi_1^{mass} + i\chi_2^{mass})$$

$$\Delta C_{20} = -(1+k_2')\frac{3}{2\sqrt{5}}\frac{C_m}{0.753R^2M}\chi_3^{mass}$$

where

R	Earth Radius	6378137 m
C_m	Earth Mantle Moment of Inertia	7.1236E+37 kg m^2
k'_2	Love number of deg 2	-0.301
M	Earth Mass	5.974E+24 kg
C-A	Differences between Polar and Equatorial Moments of Inertia	2.61E+35 kg m^2

For the CGS EOPV excitation series, with values provided at each VLBI session mid-time epochs, the daily Ocean current term and the averaged daily Atmospheric wind term excitations have been interpolated at those epochs and then removed.

The CGS EOPS excitation functions, given every three days from 1993 onwards, have been deprived of the wind term for the Atmosphere and of the current term for the Oceans at the corresponding epochs.

Assessment and comparison of C_{21}, S_{21} and C_{20} variations

The time series of ΔC_{21}, ΔS_{21} and ΔC_{20} estimated from the SLR and VLBI EOP values and those directly estimated from the SLR data analysis are shown in Figure 3. To focus on the annual and semi-annual signal components, the variations of the "motion-free" C_{21}, S_{21} and C_{20} from the SLR and VLBI EOP values, have been cleaned by linear trends, from least square adjustment, and, for C_{20}, by the low frequency terms (<1/4 cycles per year), visible in the plot of LOD excitation.

The 90-day running mean on the ΔC_{21} and ΔS_{21} residuals is compared to the respective values obtained directly from SLR dynamics, cleaned from residual Ocean/Solid Earth Pole Tide effects as explained previously and linear trends and averaged with a 90-day running mean too. All the three estimated series show similar variance for each coefficient, even with some discrepancies; an annual frequency is clearly visible in all the components, with a more significant amplitude for the S_{21} term. The variations of C_{20} show similarities too, with a residual annual signature visible in all the series.

The amplitudes of the annual and semi-annual frequencies are reported in Table 1. The values show that the ΔC_{21} estimates are very coherent among the different series: the series derived from EOPs bring to very similar values for the annual and semi-annual amplitudes.

The ΔC_{20} term from CGS DSLR, EOPS, EOPV, shows a good agreement in the annual component; it is worse, instead, in the semi-annual term. In the case of ΔC_{20}, however, the interpretation of the direct comparison of the EOP derived series with the dynamics one is a bit more complicated: the LOD derived series, after the removal of the "motion" geophysical component, has been cleaned also from the low frequency terms (<1/4 cycles per year) and compared with the de-trended ΔC_{20} from SLR dynamics.
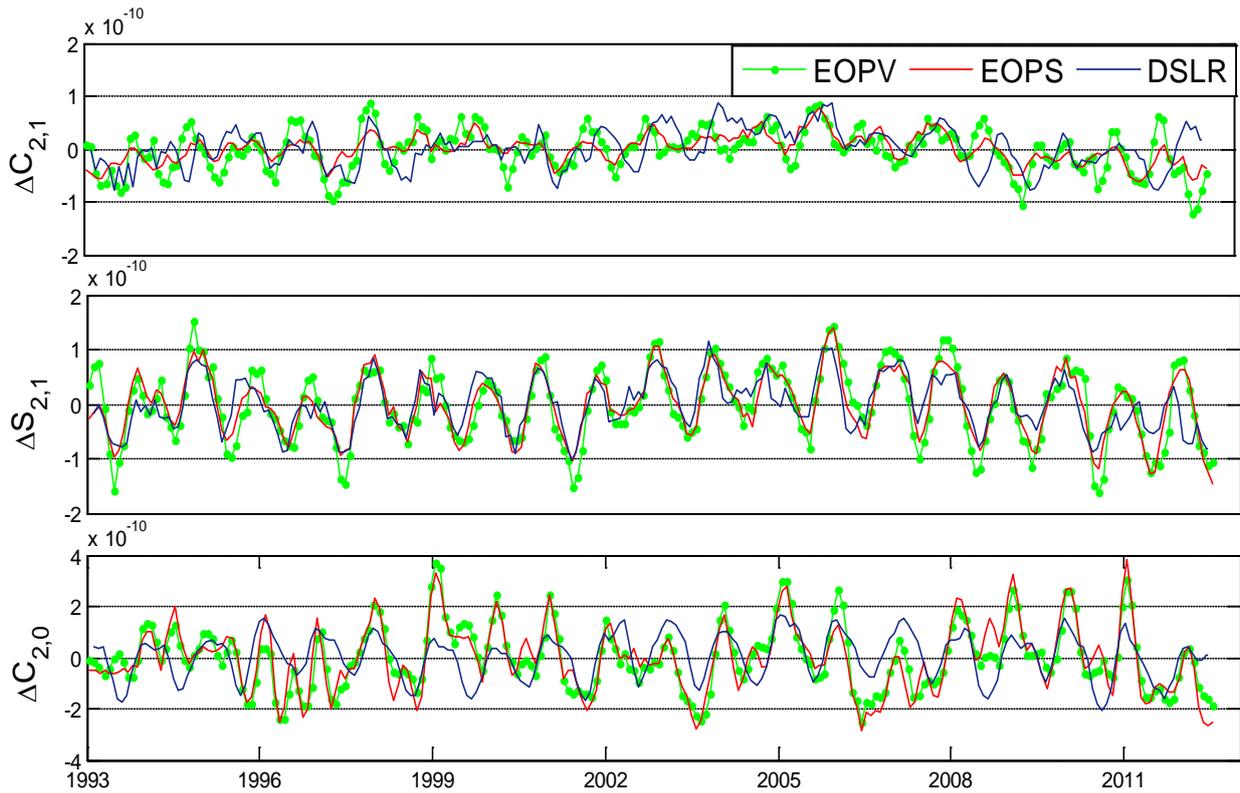
Figure 3. ΔC_{21}, ΔS_{21} and ΔC_{20} time series. EOPS is the series from SLR EOP, EOPV is the series from VLBI EOP, DSLR is the series directly estimated from SLR data

The ΔS_{21} term of the CGS EOP series shows several discrepancies both in the amplitude of the annual and semi-annual components with respect to the CGS DSLR values, which need to be investigated: the amplitude of those periodic terms from SLR Dynamics is roughly one-half of the EOP derived values.

Gravity Change	Source	Annual Amplitude [$\times 10^{-10}$]	Semiannual Amplitude [$\times 10^{-10}$]
ΔC_{21}	EOPS	0.22±0.01	0.07±0.01
	EOPV	0.30±0.02	0.06±0.02
	DSLR	0.25±0.04	0.13±0.04
ΔS_{21}	EOPS	0.71±0.02	0.21±0.02
	EOPV	0.77±0.02	0.22±0.02
	DSLR	0.48±0.05	0.11±0.05
ΔC_{20}	EOPS	1.10±0.05	1.01±0.05
	EOPV	1.16±0.05	0.99±0.05
	DSLR	1.15±0.05	0.38±0.05

Table 1. Comparison of amplitudes for the annual and semi-annual terms; EOPS, EOPV and DSLR

Conclusions

The seasonal variations (annual, semi-annual terms) in the residual time series of ΔC_{21}, ΔS_{21}, ΔC_{20} from CGS SLR dynamics (Lageos-1, Lageos-2, Starlette, Stella, Etalon-1, Etalon-2) and from CGS SLR and VLBI EOP excitation functions, evaluated on a 20-year long data set, appear to be very

similar. In particular, the agreement between the ΔC_{20}, ΔC_{21} and ΔS_{21} coefficients derived from SLR and VLBI EOPs. With respect to the SLR Dynamics values, besides a general agreement, the S_{21} term shows several discrepancies in the amplitude values of the annual and semi-annual components.

The procedure for the derivation of gravity coefficients from EOPs is rather complex. It is based on a three-step post-processing: computation of excitation functions, filtering of motion geophysical effects and, finally, conversion into values of interest. It is thus essential a very precise EOP time series, then a careful computation of the filtered series (looking for the best way to remove the geophysical motion effect from the available numerical values, including also hydrological component) and, finally, the use of coherent model values in any step throughout the procedure.

The series, deprived of the seasonal variations, can show other features, at the intra-annual and at the short period scales, useful for further investigations (as already reported in Chen and Wilson [2012]). At the intra-annual scale, the EOP values may play as very valuable climatologic monitoring for the past decades and whenever gaps exist between gravity missions.

References

Chen J.L. and C.R. Wilson, *Low degree gravitational changes from earth rotation and geophysical models*, GRL, vol. 30(24), 2257, doi: 10.1029/2003GL018688, 2003

Chen J.L., C.R. Wilson. B.D. Tapley and J.C. Ries, *Low degree gravitational changes from GRACE: Validation and interpretation*, GRL, vol. 31, L22607, 2004

Chen J.L. and C.R. Wilson, *Multi-Sensor Monitoring of Low-Degree Gravitational Changes*, Proceedings – VII Hotine-Marussi Symposium on Mathematical Geodesy, Springer Verlag, N. Sneeuw, P. Novàk, M. Crespi, F. Sansò (eds.), vol. 137 of IAG Symposia, doi: 10.1007/978-3-642-22078-4, 2012

Cheng, M.K., J.C. Ries, and B. D. Tapley, *Variations of the Earth's Figure Axis from Satellite Laser Ranging and GRACE*, J. Geophys. Res., 116, B01409, DOI:10.1029/2010JB000850, 2011

Eanes R., *A study of temporal variations in Earth's gravitational field using Lageos-1 laser range observations*, CSR-95-8, Univ. of Texas at Austin, 1995

Petit G. and B. Luzum (Eds.), IERS Conventions (2010), IERS Tech. Note 36, Bundesamt für Kartogr. und Geod., Frankfurt, Germany, 2010

Vicente R., C. Wilson, *On long-period polar motion*, Journal of Geodesy, Vol. 76, N. 4, pp. 199-208, 2002

Salstein D.A., D.M. Kann, A.J. Miller, R.D. Rosen: *The Sub-bureau for Atmospheric Angular Momentum of the International Earth Rotation Service: A Meteorological Data Center with Geodetic Applications.* Bull. Amer. Meteor. Soc., 74, 67-80, 1993

Salstein D.A., and R.D. Rosen: *Global momentum and energy signals from reanalysis systems. Preprints, 7th Conf. on Climate Variations*, American Meteorological Society, Boston, MA, 344-348, 1997

Salstein D.A., Y.H. Zhou, and J.L. Chen: *Revised angular momentum datasets for atmospheric angular momentum studies*, European Geophysical Union (EGU) Spring Meeting, Vienna, Austria, 2005

Zhou Y. H., D.A. Salstein, J.L. Chen: *Revised atmospheric excitation function series related to Earth variable rotation under consideration of surface topography*, J. Geophys. Res., 111, D12108, doi:10.1029/2005JD006608, 2006